nature physics

LETTERS

https://doi.org/10.1038/s41567-019-0546-0

Interlayer fractional quantum Hall effect in a coupled graphene double layer

Xiaomeng Liu[1], Zeyu Hao[1], Kenji Watanabe[2], Takashi Taniguchi[2], Bertrand I. Halperin[1] and Philip Kim[1*]

When a strong magnetic field is applied to a two-dimensional electron system, interactions between the electrons can cause fractional quantum Hall (FQH) effects[1,2]. Bringing two two-dimensional conductors close to each other, a new set of correlated states can emerge due to interactions between electrons in the same and opposite layers[3–6]. Here we report interlayer-correlated FQH states in a device consisting of two parallel graphene layers separated by a thin insulator. Current flow in one layer generates different quantized Hall signals in the two layers. This result is interpreted using composite fermion (CF) theory[7] with different intralayer and interlayer Chern–Simons gauge-field couplings. We observe FQH states corresponding to integer values of CF Landau level (LL) filling in both layers, as well as 'semiquantized' states, where a full CF LL couples to a continuously varying partially filled CF LL. We also find a quantized state between two coupled half-filled CF LLs and attribute it to an interlayer CF exciton condensate.

The energy levels of a non-interacting two-dimensional electron system in a magnetic field are quantized into a discrete set of Landau levels (LLs) with degeneracy proportional to the area of the system[6]. A key parameter in these systems is the LL filling factor $\nu = n\phi_0/B$, where n is the electron density, B is the magnetic field perpendicular to the layer, and the magnetic flux quantum $\phi_0 = h/e$, with $-e$ the electron charge. Integer quantized Hall effects occur when ν is an integer, where the Fermi level is in an energy gap between two LLs, and Coulomb interactions between electrons can often be ignored. However, Coulomb interactions have a dominant effect in partially filled LLs, lifting the LL degeneracy and causing new collective states of matter to appear at a certain set of fractional values of ν, which is known as the fractional quantum Hall (FQH) effect[1].

In single-layer systems, the most commonly observed FQH states can be understood in terms of the composite fermion (CF) picture[7]. Here, the electrons are each bound to an even number ($2m$) of quanta of an emergent Chern–Simons gauge field to form CFs, leaving only relatively weak residual interactions between them. Since the Chern–Simons field combines with the applied magnetic field, the CFs experience an effective magnetic field $B^* = B - 2mn\phi_0$, which is generally weaker than the original field B. From this effective magnetic field, we can relate ν to the CF LL filling factor p: $\nu = p/(2mp+1)$. If p is an integer, positive or negative, then the CF system is predicted to have an energy gap, and the electrons will be in a corresponding FQH state, with ν equal to a fraction with odd denominator. Because of this energy gap, the FQH state has vanishing longitudinal electric resistance R_{xx} and quantized Hall resistance[1] $R_{xy} = h/\nu e^2$. FQH states also have quasiparticles with fractional charge and fractional quantum statistics (anyons), different from the statistics of bosons or fermions[2,8].

The scope of quantum Hall physics further expands when we bring two layers close to each other, allowing strong Coulomb coupling between them, while suppressing a direct interlayer tunnelling. One much studied state in such systems is the interlayer-coherent integer quantum Hall state, which was first observed for the total filling factor $\nu_{tot} = 1$, where $\nu_{tot} \equiv \nu_{top} + \nu_{bot}$ is the sum of the filling factors in the top and bottom layers[5,9,10]. Due to the Coulomb interaction, electrons in one layer are correlated with holes in the other. The ground state may be described as having a Bose condensate of interlayer excitons, added to a starting state in which one layer is empty while the other has a completely full LL. As the density of excitons can be varied continuously, the interlayer-coherent state can exist over a wide range of values for the difference in layer occupations, while ν_{tot} is fixed to be an integer.

Several experimental methods, including Coulomb drag[11–13], counterflow[14,15] and tunnelling measurements[16], have been exploited to demonstrate the interlayer correlation, superfluidity and coherence of exciton condensation. In Coulomb drag measurements, current I is driven through one of the layers (drive layer), while the other layer (drag layer) is electrically not connected. When tunnelling is absent, development of a large drag voltage V_{drag} proportional to I provides direct evidence for strong interlayer correlation. For $\nu_{tot} = 1$, the Hall drag resistance $R^{xy}_{drag} = V^{xy}_{drag}/I$ is quantized to the same value as the Hall resistance of the drive layer, $R^{xy}_{drive} = R^{xy}_{drag} = h/e^2$, proving interlayer correlation and exciton superfluidity[5]. Previously, Coulomb drag studies have been exclusively performed on integer ν_{tot} exciton condensate states. In GaAs double quantum wells, $\nu_{tot} = 1$ is the only observed interlayer-correlated state, while exciton condensation at several other integer ν_{tot} values have been reported in the graphene double-layer system[12,13]. Despite theoretical expectations[6,7,17–20], no direct experimental observation of interlayer correlation at fractional total filling factor has been made thus far. The observed incompressible state at $\nu_{tot} = 1/2$ in double-layer or wide single-layer GaAs has been proposed to be the correlated Halperin (331) state[3], but without direct experimental verification[4,9,10,21]. The delicacy of these expected interlayer FQH states demands extremely high sample quality.

In the present study, we have fabricated monolayer graphene double-layer devices with top and bottom graphite gates. The heterostructure, stacked all at once, is composed of two graphene layers separated by hexagonal boron nitride (hBN), with the graphite/hBN encapsulation layers at the top and the bottom (Fig. 1d; topmost hBN layer not shown). The thickness of interlayer hBN is approximately 2.5 nm, which allows strong interlayer Coulomb interaction

[1]Department of Physics, Harvard University, Cambridge, MA, USA. [2]National Institute for Material Science, Tsukuba, Japan.
*e-mail: pkim@physics.harvard.edu

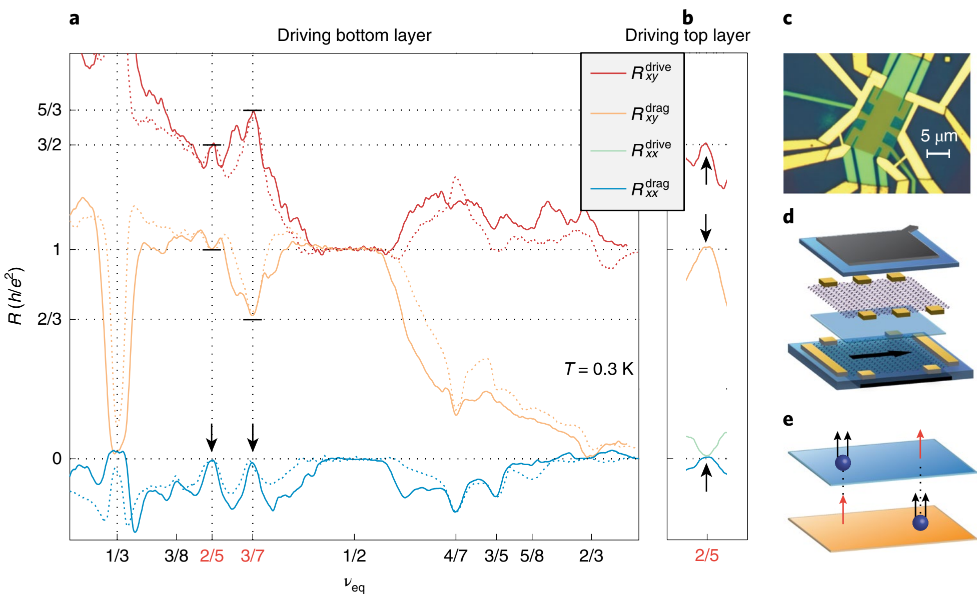

Fig. 1 | Interlayer-correlated states at fractional filling factors in graphene double layer with equal densities. **a**, Vanishing longitudinal resistance (R_{xx}^{drive}, R_{xx}^{drag}) and quantized Hall resistance (R_{xy}^{drive}, R_{xy}^{drag}) in the drive and drag layer appear at $\nu_{\mathrm{eq}}=\nu_{\mathrm{top}}=\nu_{\mathrm{bot}}=2/5$ and 3/7. The solid curves are obtained under $B=31$ T and dotted curves are from $B=25$ T. Short horizontal lines mark the Hall resistance quantization values. **b**, The same measurement as in **a** at 25 T, but with the drive and drag layers switched. **c**, Microscope image of the device. **d**, Schematic of device structure. Graphite gates are represented by black sheets while three hBN layers are shown in blue. For this specific device, the thickness of hBN between the graphene layers is 2.5 nm. Yellow blocks denote metal contacts on graphene. **e**, Illustration of Chern–Simons flux attachment. Each electron (deep blue spheres) in the system is bound with two intralayer magnetic flux quanta (black arrows) and one interlayer flux quantum (red arrows).

while preventing direct tunnel coupling between the graphene layers. The stack is then etched into a Hall bar shape and individual contacts on each layer are fabricated. No appreciable tunnelling was observed and all measurements are conducted under perpendicular magnetic fields. The top and bottom graphite gates are used to control the carrier densities of the two layers, while no interlayer bias voltage is applied. Due to the comparably reduced contact transparency for the hole doping, we focus our experiment only on the electron doping in this experiment.

Coulomb drag measurements were first performed with both layers at the same carrier density ($\nu_{\mathrm{top}}=\nu_{\mathrm{bot}}\equiv\nu_{\mathrm{eq}}$) (Fig. 1a,b). The previously observed $\nu_{\mathrm{tot}}=1$ exciton condensate state[12,13] can be clearly identified at $\nu_{\mathrm{eq}}=1/2$, with quantized $R_{xy}^{\mathrm{drive}}=R_{xy}^{\mathrm{drag}}=h/e^2$ and vanishing R_{xx}^{drag}. In this high-quality sample, however, additional features with large drag responses are also observed away from $\nu_{\mathrm{tot}}=1$, indicating that strong interlayer coupling persists, thereby enabling additional interlayer-correlated states (Fig. 1a). In particular, we observe vanishing R_{xx}^{drag} at $\nu_{\mathrm{eq}}=1/4$, 1/3, 2/5, 3/7, 2/3 (data for 1/4 is found in the Supplementary Information), which suggests that incompressible states are developed at these filling factors. Among them, $\nu_{\mathrm{eq}}=1/3$ and 2/3 appear as trivial single-layer FQH states, evident from vanishing R_{xy}^{drag}. We thus focus our attention first particularly on $\nu_{\mathrm{eq}}=2/5$ and 3/7, which are the two most prominent states that produce quantized Hall responses in the drive and drag layers. Interestingly, for these states, the two Hall resistances, R_{xy}^{drag} and R_{xy}^{drive}, are quantized to different fractional values. For $\nu_{\mathrm{eq}}=2/5$ we observe $R_{xy}^{\mathrm{drag}}=1$ and $R_{xy}^{\mathrm{drive}}=3/2$, while for $\nu_{\mathrm{eq}}=3/7$, $R_{xy}^{\mathrm{drag}}=2/3$ and $R_{xy}^{\mathrm{drive}}=5/3$ (from now on we use the unit of resistance quantum h/e^2 for the quantized resistance values). These quantization values are accurate to 1% of h/e^2 for $\nu_{\mathrm{eq}}=2/5$ and 2% for $\nu_{\mathrm{eq}}=3/7$, and stay the same for $B=25$ T and $B=31$ T. From these numbers, we note that the sum of the Hall resistances in the drive and drag layers, $R_{xy}^{\mathrm{drive}}+R_{xy}^{\mathrm{drag}}=1/\nu_{\mathrm{eq}}$, as if a portion of the Hall voltage is shifted from the drive layer to the drag layer.

We demonstrate that the $\nu_{\mathrm{eq}}=2/5$ state can be understood with a generalized CF description extended to double-layer systems. Here, we introduce multiple species of gauge field, coupling fermions in different layers as well as in the same layer. For our purposes, we attach two intralayer flux quanta and one interlayer flux quantum to each electron, so that a CF in a given layer sees two flux quanta attached to every electron in the same layer, but only one flux quantum attached to electrons in the other layer (Fig. 1e). We only work in the $|\nu_{\mathrm{top}}|$, $|\nu_{\mathrm{bot}}|<1$ region, and we assume that electrons are spin and valley polarized. By generalizing the single-layer CF picture, it is natural to define CF filling factors p_{A} and p_{B} for the top and bottom layers respectively. These are defined as the ratio between the fermion density in a given layer and the effective magnetic field felt by CFs in that layer (Supplementary Information):

$$\begin{aligned} p_{\mathrm{A}} &= \frac{\nu_{\mathrm{top}}B}{B-2n_{\mathrm{top}}\phi_0-n_{\mathrm{bot}}\phi_0} \\ &= \frac{\nu_{\mathrm{top}}}{1-2\nu_{\mathrm{top}}-\nu_{\mathrm{bot}}} \\ p_{\mathrm{B}} &= \frac{\nu_{\mathrm{bot}}}{1-2\nu_{\mathrm{bot}}-\nu_{\mathrm{top}}} \end{aligned} \quad (1)$$

Inverting equation (1), the LL filling factors for electrons in the two layers will then be given by

$$\begin{aligned} \nu_{\mathrm{top}} &= \frac{p_{\mathrm{A}}(1+p_{\mathrm{B}})}{1+2p_{\mathrm{A}}+2p_{\mathrm{B}}+3p_{\mathrm{A}}p_{\mathrm{B}}} \\ \nu_{\mathrm{bot}} &= \frac{p_{\mathrm{B}}(1+p_{\mathrm{A}})}{1+2p_{\mathrm{A}}+2p_{\mathrm{B}}+3p_{\mathrm{A}}p_{\mathrm{B}}} \end{aligned} \quad (2)$$

In the case where the layers have equal densities, this formula simplifies to $\nu_{\mathrm{eq}}=p/(3p+1)$, where $p=p_{\mathrm{A}}=p_{\mathrm{B}}$.

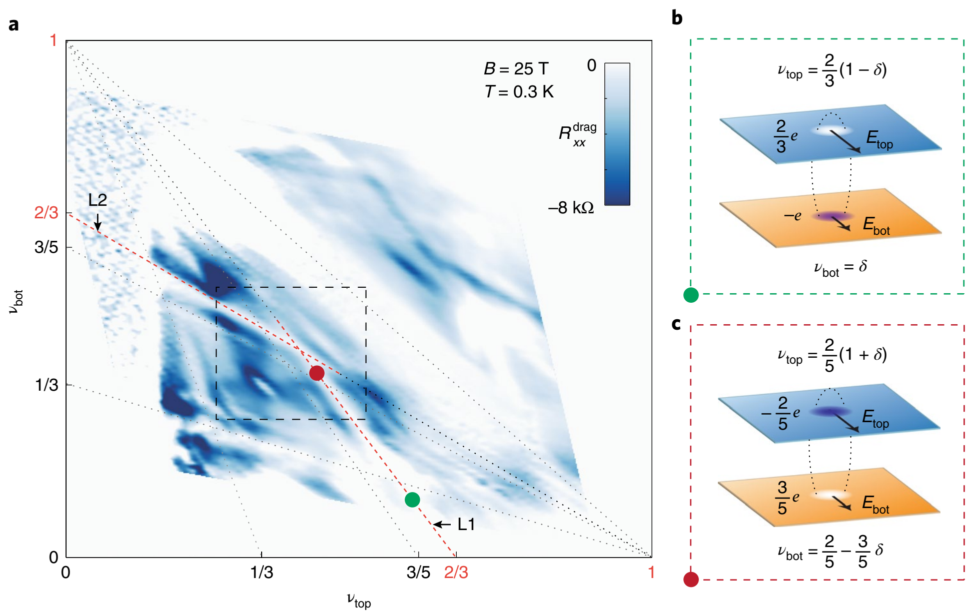

Fig. 2 | Interlayer correlation through quasiparticle pairing. a, Longitudinal drag resistance as a function of filling factors in the top and bottom layers. Dotted lines show locations of semiquantized states where longitudinal drag resistance vanishes. All these lines connect $\nu = 1$ in one layer with various $\nu = 1/3$, 3/5, 2/3, 1 of the other layer. Among them, the intersection of red dotted lines marked by L1 and L2 corresponds to the $\nu_{eq} = 2/5$ state discussed above. The dashed rectangle denotes the scope of the magnified measurements of Fig. 3. **b**,**c**, Illustrations of quasiparticle pairing for two filling-factor configurations (green and red dots in **a**). The circles on the two graphene layers represent quasiparticle excitations with marked electrical charges ($-e$, $2/3e$, …). These quasiparticle pairs are balanced by the transverse electrical fields on the top and bottom layers (E_{top} and E_{bot}, depicted by black arrows).

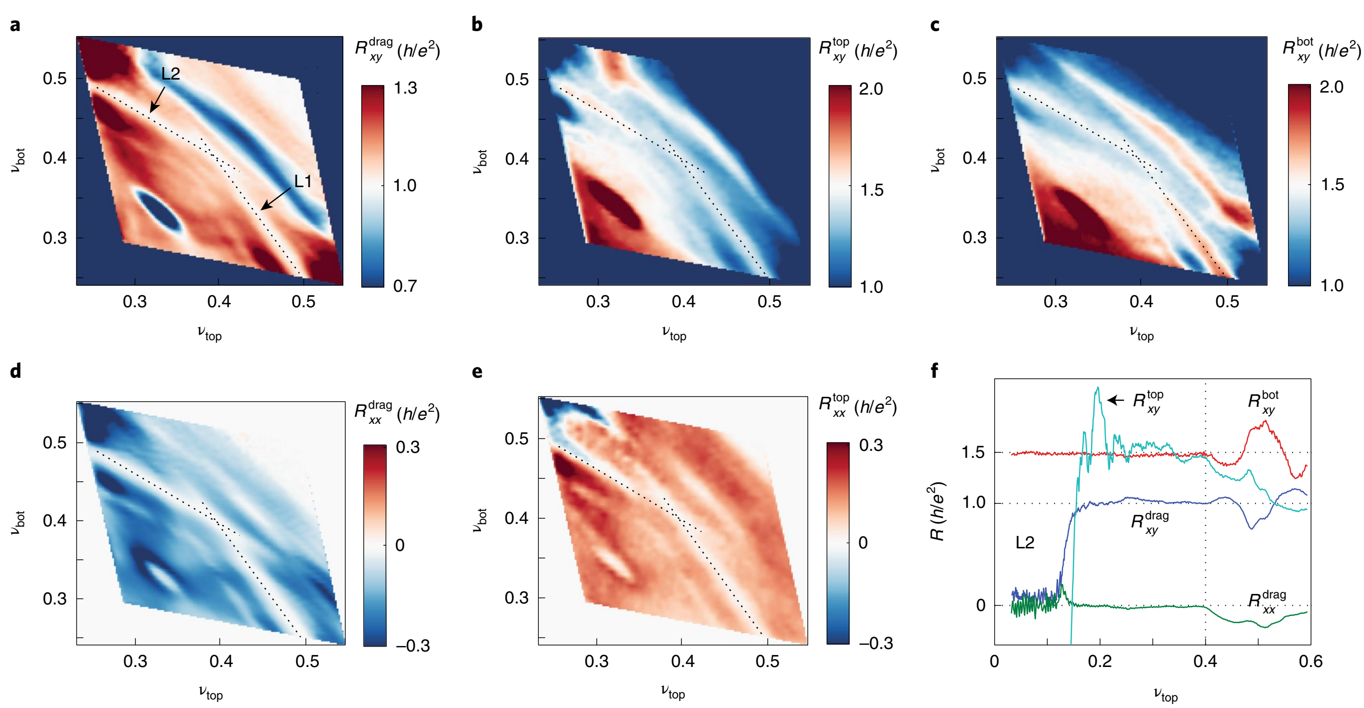

Fig. 3 | Semiquantized fractional Hall states. a–e, Various resistance measurements in the magnified area indicated by the dashed rectangle in Fig. 2. $R_{xx,xy}^{top}$ ($R_{xx,xy}^{bot}$) is the drive layer resistance when the current is driven on the top (bottom) layer. The dotted lines mark L1 and L2 (the same as the red lines in Fig. 2). Along L1, quantum Hall signatures ($R_{xx}^{top} = 0$, $R_{xy}^{top} = 3h/2e^2$) persist on the top layer but not on the bottom layer ($R_{xx}^{bot} \neq 0$, $R_{xy}^{top} \neq 3h/2e^2$), while the opposite is true for L2. Meanwhile, drag signals are quantized along both L1 and L2. **f**, Line cut through L2. It is notable that R_{xy}^{bot} remained constant all the way until $\nu_{eq} = 2/5$ (vertical dotted line), across the phase transition between the single-layer $\nu_{bot} = 2/3$ FQH state ($R_{xy}^{drag} \approx 0$) and the interlayer FQH state ($R_{xy}^{drag} = h/e^2$).

Table 1 | Resistance response of semiquantized states

	R_{xx}^{drag}	R_{xy}^{drag}	R_{xx}^{top}	R_{xy}^{top}	R_{xx}^{bot}	R_{xy}^{bot}
L1	0	1	0	1.5	≠0	non-quantized
L2	0	1	≠0	non-quantized	0	1.5

Summary of resistance behaviour (in units of h/e^2) along L1 and L2 shown in Fig. 2.

The experimentally observed interlayer-correlated state $\nu_{\text{eq}}=2/5$ corresponds to $p_{\text{A}}=p_{\text{B}}=-2$. Since the CFs in the two layers are correlated, the Hall signal in the two layers must be correlated as well. Using the Chern–Simons field calculation, we find that the double-layer Hall resistivity tensor obeys (see Supplementary Information for derivation)

$$\hat{\rho}_{xy}\equiv\begin{pmatrix}\rho_{xy}^{\text{top}} & \rho_{xy}^{\text{drag}}\\ \rho_{xy}^{\text{drag}} & \rho_{xy}^{\text{bot}}\end{pmatrix}=\hat{\rho}_{\text{CS}}+\hat{\rho}_{\text{cf}}=\begin{pmatrix}2 & 1\\ 1 & 2\end{pmatrix}+\begin{pmatrix}1/p_{\text{A}} & 0\\ 0 & 1/p_{\text{B}}\end{pmatrix} \quad (3)$$

In this equation, $\hat{\rho}_{xy}$ is the Hall resistivity matrix in the unit of the resistance quantum, which contains two contributing terms: $\hat{\rho}_{\text{CS}}$ originates from the motion of the Chern–Simons flux considering the two intralayer flux quanta and one interlayer flux quantum, while $\hat{\rho}_{\text{cf}}$ is caused by the Hall effect of CFs. At $\nu_{\text{eq}}=2/5$, equation (3) produces $R_{xy}^{\text{drag}}=1$ and $R_{xy}^{\text{drive}}=3/2$, matching the experimental observations in Fig. 1a,b.

Applying CF formalism similar to that discussed above (equation (1)) to $\nu_{\text{eq}}=3/7$, however, we obtain $p_{\text{A}}=p_{\text{B}}=-3/2$, indicating that two half-filled CF LLs are involved in this state. A half-filled CF LL by itself should not develop an incompressible state. Moreover, if we were to enforce equation (3) for these values of p_{A} and p_{B}, we would predict $\rho_{xy}^{\text{drag}}=1$ and $\rho_{xy}^{\text{drive}}=4/3$, which is in strong disagreement with the experimentally observed values, 2/3 and 5/3, respectively.

To correct the weakly interacting CF model presented above for half-filled CF LLs, we can draw an analogy between the half-filled CF double-layer system and the half-filled electron double-layer system, in which an exciton condensate can be formed. If we assume pairing between CFs in one layer and CF holes in the second layer, the CF Hall resistivity tensor becomes

$$\hat{\rho}_{\text{cf}}=\frac{1}{p_{\text{A}}+p_{\text{B}}}\begin{pmatrix}1 & 1\\ 1 & 1\end{pmatrix} \quad (4)$$

Inserting equation (4) into equation (3), we obtain $R_{xy}^{\text{drag}}=2/3$ and $R_{xy}^{\text{drive}}=5/3$, which agrees with our experimental observations, thus suggesting that the CF exciton condensation phase is indeed responsible for $\nu_{\text{eq}}=3/7$ (further discussion of CF paring in half-filled CF LLs can be found in the Supplementary Information).

Away from equal filling status, Fig. 2a shows that the vanishing R_{xx}^{drag} persists along the segments of two symmetric lines (labelled L1 and L2) that intersect at $\nu_{\text{eq}}=2/5$. The line L2 has a slope of −2/3 and traces from $(\nu_{\text{top}},\nu_{\text{bot}})=(0,2/3)$ to (1,0), while L1 is the inverse. We find that the longitudinal drag vanishes and Hall drag remains quantized along these lines, as shown in Fig. 3a,d, indicating that the strong interlayer interaction persists along these line segments. Unlike the quantized interlayer drag resistance, which is layer independent by the Onsager relation, we find that the drive Hall resistance depends on which layer we measure. For example, along L2, we find that driving the bottom layer exhibits a quantum Hall effect with $R_{xy}^{\text{bot}}=3/2$ and $R_{xx}^{\text{bot}}=0$. However, when we drive the top layer along L2, $R_{xx}^{\text{top}}>0$ and R_{xy}^{top} is not quantized. Along L1, the role of the top and bottom layers is reversed. The experimentally observed behaviours of all the resistance components along L1 and L2 are summarized in Table 1.

We note that, along L1 or L2, either p_{A} or p_{B} remains at −2 while the other can change continuously. For example, for $p_{\text{B}}=-2$, ν_{top} and ν_{bot} given by equation (2) satisfy the expression of L2: $\left(\nu_{\text{top}}+\frac{3}{2}\nu_{\text{bot}}=1\right)$. In principle, a series of discrete incompressible FQH states can be formed along this line, corresponding to various positive and negative integer values for p_{A} in equation (2). These should all exhibit vanishing longitudinal resistance and quantized $R_{xy}^{\text{drag}}=1$ and $R_{xy}^{\text{bot}}=3/2$, which do not depend on p_{A}, while the quantized values of R_{xy}^{top} would depend on the value of p_{A}. What originally surprised us, however, is that the experimentally observed quantization of $R_{xy}^{\text{drag}}=1$ and $R_{xy}^{\text{bot}}=3/2$, together with vanishing R_{xx}^{drag} and R_{xx}^{bot}, exists continuously along an entire segment of L2, even when p_{A} is not an integer.

We now understand the above results as follows. For a general point on the line segment L2 (that is, fixed $p_{\text{B}}=-2$), there is an energy gap for adding or removing a CF of type B (δp_{B}), but not of type A (δp_{A}). Thus, while the state should not be as stable as at a point where p_{A} and p_{B} are both integers, such that both species of CF are gapped, it should nevertheless be more stable than at a nearby point where both CF filling factors are fractions. Therefore, it is plausible that CF states along a line where one of (p_{A}, p_{B}) is an integer should be good candidates for the true ground state at the corresponding filling fractions. We call such states semiquantized, as one CF filling factor is fixed but the other can vary continuously. The observed transport properties of these states can be understood with the CF picture as well (Methods).

An alternative approach to understanding properties of the states along L1 and L2 is to begin with the balanced quantized state at $\nu_{\text{eq}}=2/5$, and add quasiholes to this state. Elementary quasiholes in this state have total charge $e/5$, with $3e/5$ in one layer and $-2e/5$ in the other. The addition of one type of quasihole or the other will move the system along the line L1 or L2, in a direction decreasing the total filling factor. The relative stability of states on the two line segments can be understood by considering the energy cost for quasiholes versus quasiparticles (see the Supplementary Information for more discussion).

Finally, we turn to the state at $\nu_{\text{eq}}=1/4$ and the lines through it. The state $\nu_{\text{eq}}=1/4$ may be described in our CF language by $p_{\text{A}}=p_{\text{B}}=1$. As discussed in the Supplementary Information, the state is also equivalent to the Halperin (331) state, which has been proposed as a possible explanation for the FQH state at $\nu_{\text{tot}}=1/2$ in wide GaAs quantum wells. The line L3 in Supplementary Fig. 2, which passes through this point, corresponds to $p_{\text{A}}=1$ with continuously varying p_{B}. Although there appears to be a well developed FQH state at $p_{\text{B}}=2$ with $p_{\text{A}}=1$ along this line, corresponding to the values $\nu_{\text{top}}=3/13$, $\nu_{\text{bot}}=4/13$, there does not appear to be a line of semiquantized states between these two points. The absence of continuous semiquantization along these lines suggests that stabilization of the interlayer-correlated CF state requires microscopic consideration of the energetics of the quasiparticle addition to the system (Supplementary Information).

Online content

Any methods, additional references, Nature Research reporting summaries, source data, statements of code and data availability and associated accession codes are available at https://doi.org/10.1038/s41567-019-0546-0.

Received: 19 October 2018; Accepted: 2 May 2019;
Published online: 24 June 2019

References

1. Tsui, D. C., Stormer, H. L. & Gossard, A. C. Two-dimensional magnetotransport in the extreme quantum limit. *Phys. Rev. Lett.* **48**, 1559–1562 (1982).
2. Laughlin, R. B. Anomalous quantum Hall effect: an incompressible quantum fluid with fractionally charged excitations. *Phys. Rev. Lett.* **50**, 1395–1398 (1983).

3. Halperin, B. I. Theory of the quantized Hall conductance. *Helv. Phys. Acta* **56**, 75–104 (1983).
4. Chakraborty, T. & Pietiläinen, P. Fractional quantum Hall effect at half-filled Landau level in a multiple-layer electron system. *Phys. Rev. Lett.* **59**, 2784–2787 (1987).
5. Eisenstein, J. Exciton condensation in bilayer quantum Hall systems. *Annu. Rev. Condens. Matter Phys.* **5**, 159–181 (2014).
6. Jain, J. *Composite Fermions* (Cambridge Univ. Press, 2007).
7. Jain, J. K. Composite-fermion approach for the fractional quantum Hall effect. *Phys. Rev. Lett.* **63**, 199–202 (1989).
8. Halperin, B. I. Statistics of quasiparticles and the hierarchy of fractional quantized Hall states. *Phys. Rev. Lett.* **52**, 1583–1586 (1984).
9. Suen, Y. W., Engel, L. W., Santos, M. B., Shayegan, M. & Tsui, D. C. Observation of a $\nu = 1/2$ fractional quantum Hall state in a double-layer electron system. *Phys. Rev. Lett.* **68**, 1379–1382 (1992).
10. Eisenstein, J. P., Boebinger, G. S., Pfeiffer, L. N., West, K. W. & He, S. New fractional quantum Hall state in double-layer two-dimensional electron systems. *Phys. Rev. Lett.* **68**, 1383–1386 (1992).
11. Kellogg, M., Spielman, I. B., Eisenstein, J. P., Pfeiffer, L. N. & West, K. W. Observation of quantized Hall drag in a strongly correlated bilayer electron system. *Phys. Rev. Lett.* **88**, 126804 (2002).
12. Liu, X., Watanabe, K., Taniguchi, T., Halperin, B. I. & Kim, P. Quantum Hall drag of exciton condensate in graphene. *Nat. Phys.* **13**, 746–750 (2017).
13. Li, J. I., Taniguchi, T., Watanabe, K., Hone, J. & Dean, C. R. Excitonic superfluid phase in double bilayer graphene. *Nat. Phys.* **13**, 751–755 (2017).
14. Kellogg, M., Eisenstein, J. Pv, Pfeiffer, L. N. & West, K. W. Vanishing Hall resistance at high magnetic field in a double-layer two-dimensional electron system. *Phys. Rev. Lett.* **93**, 036801 (2004).
15. Tutuc, E., Shayegan, M. & Huse, D. A. Counterflow measurements in strongly correlated GaAs hole bilayers: evidence for electron-hole pairing. *Phys. Rev. Lett.* **93**, 036802 (2004).
16. Spielman, I. B., Eisenstein, J. P., Pfeiffer, L. N. & West, K. W. Resonantly enhanced tunneling in a double layer quantum Hall ferromagnet. *Phys. Rev. Lett.* **84**, 5808–5811 (2000).
17. Yoshioka, D., MacDonald, A. H. & Girvin, S. M. Fractional quantum Hall effect in two-layered systems. *Phys. Rev. B* **39**, 1932–1935 (1989).
18. Scarola, V. W. & Jain, J. K. Phase diagram of bilayer composite fermion states. *Phys. Rev. B* **64**, 085313 (2001).
19. Barkeshli, M. & Wen, X.-G. Non-Abelian two-component fractional quantum Hall states. *Phys. Rev. B* **82**, 233301 (2010).
20. Geraedts, S., Zaletel, M. P., Papić, Z. & Mong, R. S. K. Competing Abelian and non-Abelian topological orders in $\nu = 1/3 + 1/3$ quantum Hall bilayers. *Phys. Rev. B* **91**, 205139 (2015).
21. He, S., Das Sarma, S. & Xie, X. C. Quantized Hall effect and quantum phase transitions in coupled two-layer electron systems. *Phys. Rev. B* **47**, 4394–4412 (1993).

Acknowledgements

The major experimental work is supported by DOE (DE-SC0012260). The theoretical analysis was supported by the Science and Technology Center for Integrated Quantum Materials, NSF grant no. DMR-1231319. P.K. acknowledges partial support from the Gordon and Betty Moore Foundation's EPiQS Initiative through grant GBMF4543. K.W. and T.T. acknowledge support from the Elemental Strategy Initiative conducted by MEXT, Japan, and CREST(JPMJCR15F3), JST. A portion of this work was performed at the National High Magnetic Field Laboratory, which is supported by the National Science Foundation Cooperative Agreement no. DMR-1157490* and the State of Florida. Nanofabrication was performed at the Center for Nanoscale Systems at Harvard, supported in part by NSF NNIN award ECS-00335765. In preparation of this manuscript, we are aware of related work done by J. I. A. Li et al. We thank B. Rosenow, J. I. A. Li and C. Dean for helpful discussions.

Author contributions

X.L. and P.K. conceived the experiment. X.L. and Z.H. fabricated the samples and performed the measurements. X.L. analysed the data. B.H. conducted the theoretical analysis. X.L., B.I.H. and P.K. wrote the paper. K.W. and T.T. supplied hBN crystals.

Competing interests

The authors declare no competing interests.

Additional information

Supplementary information is available for this paper at https://doi.org/10.1038/s41567-019-0546-0.

Reprints and permissions information is available at www.nature.com/reprints.

Correspondence and requests for materials should be addressed to P.K.

Peer review information: *Nature Physics* thanks Timo Hyart, Emanuel Tutuc and the other, anonymous, reviewer(s) for their contribution to the peer review of this work.

Publisher's note: Springer Nature remains neutral with regard to jurisdictional claims in published maps and institutional affiliations.

Methods

Sample fabrication. The hBN–graphite–hBN–graphene–hBN–graphene–hBN–graphite (from top to bottom) stack is prepared by mechanical exfoliation and the van der Waals transfer technique. The dual graphite gates shield the graphene layers from impurities and contaminations, enabling lower disorder and more homogeneous samples[22]. The shapes of the graphene and graphite are carefully chosen and arranged so that we can use the overlapping part as the main channel area, while fabricating individual contacts on each layer in the regions with just one conducting layer. A square-shaped top graphene layer is chosen, while we pick strip-shaped bottom graphene and bottom graphite layers, which are narrower but longer than the top graphene. We align the bottom graphite and bottom graphene layers into a cross, while keeping the overlapping area inside the top graphene square. The top graphite layer covers everything after stacking but is etched into the same shape as the bottom graphite layer. We then etch the stack into the final device geometry and fabricate the Cr/Pd/Au contact on all the graphene and graphite layers. Contacts on the two layers are spatially separated to avoid shorting the two graphene layers together[12]. Finally, we grow 20–30 nm atomic layer deposited Al_2O_3, and then deposit contact gates above the top-layer graphene lead to increase the contact transparency.

Coulomb drag measurement. We perform Coulomb drag measurement with 2 nA excitation current on the drive layer using lock-in amplifiers at 17.7 Hz. We use a symmetric bias scheme to eliminate any possible interlayer bias effect[12,23,24]. In this scheme, we apply positive bias $+V$ on the source and $-V$ on the drain (both on the drive layer). The drag layer is open circuit but with one of the contacts connected to the ground through a 1 MΩ resistor to allow charges to flow in and out of the layer for the gating effect. Using an atomic layer deposited contact gate and a silicon back gate, we dope the lead area of both layers to high carrier density and matching carrier type with the channel. The measurements are made in a helium-3 cryostat at 300 mK. The filling factors presented are calculated from gate voltages with gate capacitance calibrated by gate voltages of sharp single-layer quantum Hall states $\nu_{\rm top}=\nu_{\rm bot}=1/3$ and $\nu_{\rm top}=\nu_{\rm bot}=2/3$, and are reasonably well matched with measured hBN thickness. The perpendicular electric field generated by the gate voltages has no effect in the case of a monolayer graphene double layer.

Understanding transport properties of semiquantized states. To understand transport properties in a semiquantized state, we first note that in the absence of CF scattering or of pinning by impurities there would be no longitudinal resistance and the Hall resistances would be given by equation (3), even in the absence of an energy gap. For the semiquantized state along L2 ($p_{\rm B}=-2$), if an electrical current is driven on the bottom layer, then the current can be carried entirely by CFs of type B (bottom drive), with stationary CFs of type A (top, drag layer). Since type B CFs are contained in a filled CF LL, the current is carried without dissipation. Furthermore, as there is no tendency for flow of the type A CFs, a small density of impurities will have no effect, leading to quantization $\rho_{xy}^{\rm bot}=3/2$ and $\rho_{xy}^{\rm drag}=1$. On the other hand, if current is applied to the top layer, CFs of type A will be forced to move. If CFs in the partially filled CF LL are not pinned by impurities, they will participate in the motion, and they can be scattered by impurities. This will lead to a longitudinal resistance, and deviations from the result $R_{xy}^{\rm top}=(2+1/p_{\rm A})$ predicted by equation (3), except in the case where $p_{\rm A}$ is so close to an integer value that the small density of excess CFs is pinned by impurities.

Data availability

The data that support the plots within this paper and other findings of this study are available from the corresponding author on reasonable request.

References

22. Zibrov, A. A. et al. Tunable interacting composite fermion phases in a half-filled bilayer-graphene Landau level. *Nature* **549**, 360–364 (2017).
23. Kellogg, M. J. *Evidence for Excitonic Superfluidity in a Bilayer Two-Dimensional Electron System*. PhD thesis, California Institute of Technology (2005).
24. Hill, N. P. R. et al. Frictional drag between parallel two-dimensional electron gases in a perpendicular magnetic field. *J. Phys. Condens. Matter* **8**, L557–L562 (1996).